Hindawi
Advances in Materials Science and Engineering
Volume 2018, Article ID 7320298, 11 pages
https://doi.org/10.1155/2018/7320298

Research Article

Utilization of Sandy Soil as the Primary Raw Material in Production of Unfired Bricks

Guilan Tao[1,2] **Yuepeng Pan**[1,2] **Zhaoyang Qiao**[1,2] **and Chaohua Jiang**[1,2]

[1]*Jiangsu Key Laboratory of Coast Ocean Resources Development and Environment Security, Hohai University, Nanjing 210098, China*
[2]*College of Harbour, Coastal and Offshore Engineering, Hohai University, Nanjing 210098, China*

Correspondence should be addressed to Chaohua Jiang; chaohuajiang@hhu.edu.cn

Received 29 May 2017; Revised 25 November 2017; Accepted 5 December 2017; Published 5 February 2018

Academic Editor: Giorgio Pia

In this study, attempts were made to use sandy soil as the main raw material in making unfired bricks. The sprayed-cured brick specimens were tested for compressive and flexural strength, rate of water absorption, percentage of voids, bulk density, freezing/thawing, and water immersion resistance. In addition, the microstructures of the specimens were also studied using scanning electron microscope (SEM) and X-ray diffraction (XRD) technique. The test results show that unfired brick specimens with the addition of ground-granulated blast-furnace slag (GGBS) tend to achieve better mechanical properties when compared with the specimens that added cement alone, with GGBS correcting particle size distribution and contributing to the pozzolanic reactions and the pore-filling effects. The test specimens with the appropriate addition of cement, GGBS, quicklime, and gypsum are dense and show a low water absorption rate, a low percentage of voids, and an excellent freezing/thawing and water immersion resistance. The SEM observation and XRD analysis verify the formation of hydrate products C–S–H and ettringite, providing a better explanation of the mechanical and physical behavior and durability of the derived unfired bricks. The results obtained suggest that there is a technical approach for the high-efficient comprehensive utilization of sandy soil and provide increased economic and environmental benefits.

1. Introduction

In the context of environmental protection and sustainable development, the beneficial use of waste soil such as clay soil and sandy soil in civil engineering has gained more and more acceptance in many countries. More recently, there has been a growing interest in producing unfired bricks from recycled waste and by-product materials from the industry [1–5]. Compared with conventional fired clay bricks and ordinary Portland cement (OPC) concrete bricks, the production of unfired bricks from waste materials can significantly reduce the consumption of energy and emission of greenhouse gases [6]. Furthermore, without using clay soil or firing in high temperature, unfired bricks made with sandy soil can avoid an adverse effect on the landscape and generating high level of wastes [7]. Because of these advantages, the replacement of fired clay bricks and OPC concrete bricks with unfired bricks in construction is highly desirable, especially in the places where there is a shortage of natural resources such as clay soil and coarse aggregate.

In order to obtain the best performance, it is necessary to carefully establish the type and quantity of the used additives and the optimum water content [8]. Extensive research has been conducted on making unfired bricks from a wide variety of waste and by-product materials such as fly ash, GGBS, lime, or different cement mixtures [9]. Roy et al. [10] used gold mill tailings to make bricks by mixing them with OPC. The compressive strength test results of water-cured cement-tailing bricks showed that bricks with 20% cement and 14 days of curing were found to be suitable. Malhotra and Tehri [11] investigated the compressive strength (in saturated conditions), bulk density, and water absorption properties of bricks from GGBS and found that good-quality bricks could be produced from a slag-lime-sand mixture.

Table 1: The chemical compositions and the physical properties of OPC, GGBS, and sandy soil.

Chemical composition (wt.%)	Cement (OPC)	GGBS	Sandy soil
CaO	62.25	37.04	8.54
SiO_2	20.58	32.90	68.73
Al_2O_3	5.64	15.36	11.33
Fe_2O_3	3.95	2.46	3.82
MgO	2.48	10.18	3.02
Na_2O	3.18	1.12	1.46
K_2O	0.36	0.15	2.00
SO_3	0.32	0.08	0.05
TiO_2	—	—	0.65
Loss on ignition	—	0.38	—
Physical properties			
Specific gravity (g/cm^3)	3.10	2.84	2.33
Specific surface (m^2/kg)	365	425	—
Initial setting time (min)	138	—	—
Final setting time (min)	204	—	—
Fineness modulus	—	—	0.82

Kumar [12] studied the production of bricks and hollow blocks using class F fly ash together with calcined phosphogypsum and mineral lime, which showed that these bricks and hollow blocks had sufficient strength for their use in low-cost housing development [13]. It has been found that through adding waste and by-product materials, unfired bricks showed a marked improvement in performance and were suitable to be utilized as building materials.

As one kind of waste materials, sandy soil is available in huge quantities in coastal rivers such as Yangtze River and Yellow River and in desert areas. After waterway regulation engineering, a great amount of waste sandy soil is abandoned and covers a large area of the land near the river. The transportation of sandy soil also increases the costs of engineering. Sandy soil, at present, is mainly applied in roadbed reinforcement and foundation treatment, for it has the features of poor gradation, low strength, looseness, ease of erosion, and the poor overall stability [14, 15]. Great economic and environmental benefits will be brought if measures can be taken to utilize this sandy soil to produce facing bricks and ballast blocks used in the local waterway regulation engineering, because problems caused by this kind of sandy soil such as land taking, high cost of transportation, and pollution can be avoided. On the other hand, in all the reported studies on the possible utilization of waste and by-product materials for building brick production, the information about preparing unfired bricks with sandy soil is very limited. Therefore, to utilize sandy soil as the main raw material for unfired brick preparation, further studies need to be carried out, which provides a technical approach for the high-efficient comprehensive utilization of sandy soil.

This paper aims at developing the possibility of unfired bricks made with waste sandy soil from waterway regulation engineering. This research was designed to address the following main objectives: (1) to investigate the compressive and flexural strength of the unfired bricks, (2) to investigate the water absorption, percentage of voids, and bulk density of the unfired bricks, and (3) to assess the durability of the unfired bricks by means of repeated freezing/thawing cycles and water immersion aging. The characterization of the microstructure such as SEM observation and XRD analysis that is responsible for the change in behavior of the derived unfired bricks is also reported.

2. Materials and Methods

2.1. Materials

2.1.1. Cement. In this study, ordinary Portland cement was obtained from the Conch Cement Pty. Ltd., China. The chemical compositions determined according to Chinese National Standard GB 175-2007 and the properties of OPC are presented in Table 1.

2.1.2. GGBS. In this study, GGBS supplied by a construction company located in Nanjing of China was used as mineral admixture. The chemical compositions and physical properties of GGBS are illustrated in Table 1.

2.1.3. Quicklime and Gypsum. The quicklime used is provided by Shanghai JiuYi Chemical Reagent Pty. Ltd. The gypsum used is industrial α-dehydrated gypsum powder provided by Chengdu KeLong Chemical Reagent Factory in China, among which the content of $Ca_2SO_4{\cdot}2H_2O$ is more than 97.1%.

2.1.4. The Sandy Soil. The sandy soil was collected from natural soil deposits along the Yangtze River in China. After collection, the sandy soil was air-dried and sieved to <2 mm. The grain size distribution of the sandy soil was determined using the dry sieve analysis method and is presented in

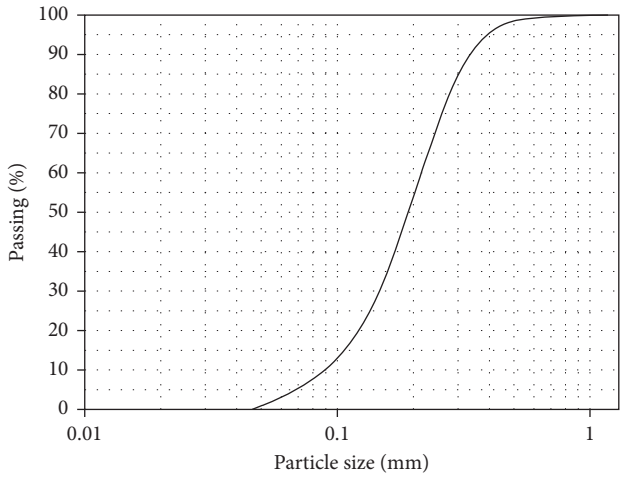

Figure 1: Grain size distributions of the used sandy soil.

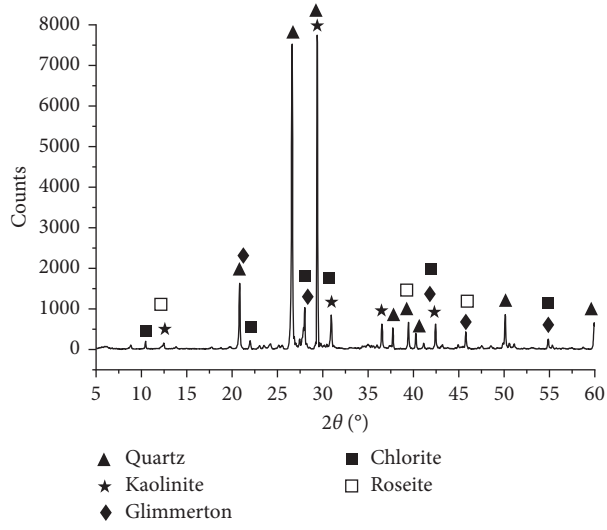

Figure 2: XRD diagram of the used sandy soil.

Table 2: Mix proportions of specimens by weight and the mix code.

Mix code	Sandy soil (wt.%)	Cement (wt.%)	GGBS (wt.%)	Quicklime (wt.%)	Gypsum (wt.%)	Water/solid ratio
C25	75	25	—	—	—	0.125
C20GG5	75	20	5	—	—	0.125
C15GG10	75	15	10	—	—	0.125
C10GG10Q5	75	10	10	5	—	0.125
C8GG10Q5G2	75	8	10	5	2	0.125
C8GG10Q3G4	75	8	10	3	4	0.125

Figure 1. This soil can be classified as sandy soil according to GB/T50145-2007. The chemical compositions and physical properties of the sandy soil are presented in Table 1. The mineralogical compositions of the sandy soil are determined by XRD analysis using Ultima IV made in Japan. The XRD results are shown in Figure 2. The main minerals are quartz, kaolinite, glimmerton, chlorite, and roseite.

2.2. Mix Proportions. Table 2 reports the details of the mix proportions. For all mixtures, the fixed sandy soil is 75% of solid materials and water/solid ratio is 0.125.

2.3. Preparation and Curing Conditions of Specimens. All specimens were prepared with static compaction method.

The dry sandy soil, cement, GGBS, quicklime, and gypsum were initially mixed in a mixer for about 2 minutes until they were homogenous thoroughly. Then, the appropriate amount of water was added and the mixing process lasted for another 3 minutes. The prepared mixture was immediately cast in the molds and compacted by the universal testing machine. The compaction specimens were prepared at an automatically controlled loading pressure of 400 N/s and stopped when the pressure reached 20 MPa. The compacted specimens were immediately removed from the molds and were cured in the normal lab environment of $20 \pm 5^{\circ}C$ and $50 \pm 15\%$ relative humidity, being sprinkled by water to be damped twice a day in the first 7 days and then once a day until the age of 28 days. In this study, every reported test result consists of the average of 3 replicate tests except 5 specimens for freezing/thawing cycles.

2.4. Testing Methods

2.4.1. Compressive and Flexural Strength. The compressive strength and flexural strength of the specimens with size of 240 mm × 105 mm × 53 mm were tested according to Chinese National Standard GB/T 4111-2013, after 7, 28, and 90 days of curing.

2.4.2. Water Absorption Rate. Some of the test specimens were dried to a constant mass and allowed to cool until an ambient temperature in accordance with GB/T 4111-2013. After being immersed in a water tank for 24 hours, the specimens were removed out, and the surface water was wiped off with a damp cloth.

2.4.3. Percentage of Voids. The percentage of the voids test was conducted according to GB/T 4111-2013. In the test, the voids percentage of each specimen was determined by hydrostatic weighing, and the values were recorded.

2.4.4. Bulk Density. The bulk density (unit weight) of the prepared bricks was determined using GB/T 4111-2013.

2.4.5. Freezing/Thawing Cycles. The freezing/thawing test was carried out according to GB/T 4111-2013 method. The compressive strength and weight loss were measured every five cycles and compared with the values before the freezing/thawing cycles.

2.4.6. Water Immersion. The water immersion test was performed according to GB/T 4111-2013. After 28 days of curing, specimens were immersed in $20 \pm 5^{\circ}C$ water for 4 days. After that, all specimens were subject to compressive strength test.

2.4.7. Microstructure Analysis. The microstructure of C8GG10Q5G2 (the optimum) cured for 7 and 28 days was tested by JSM-5900 SEM made of the JEOL of Japan. The crystalline phases of C8GG10Q5G2 cured for 7, 28, and 90 days were analyzed by XRD using Cu-Kα radiation, with the peaks identified by means of the International Centre for Diffraction Data (ICDD) standard database.

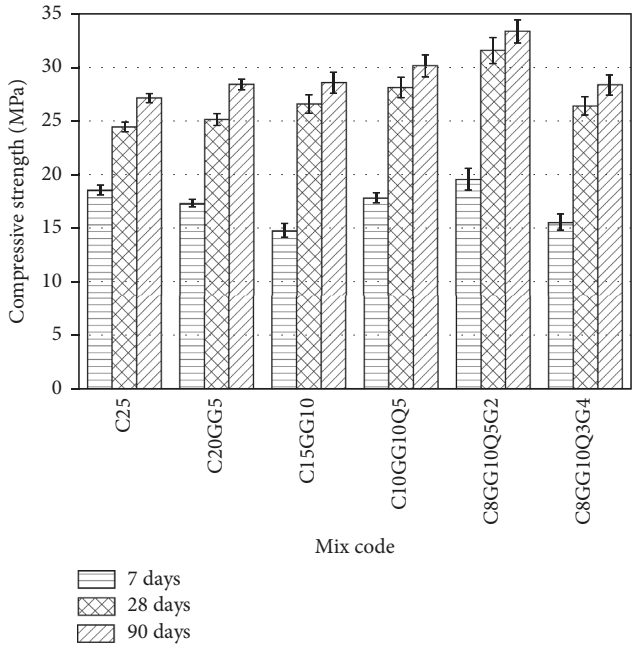

Figure 3: Development of compressive strength of designed mixes.

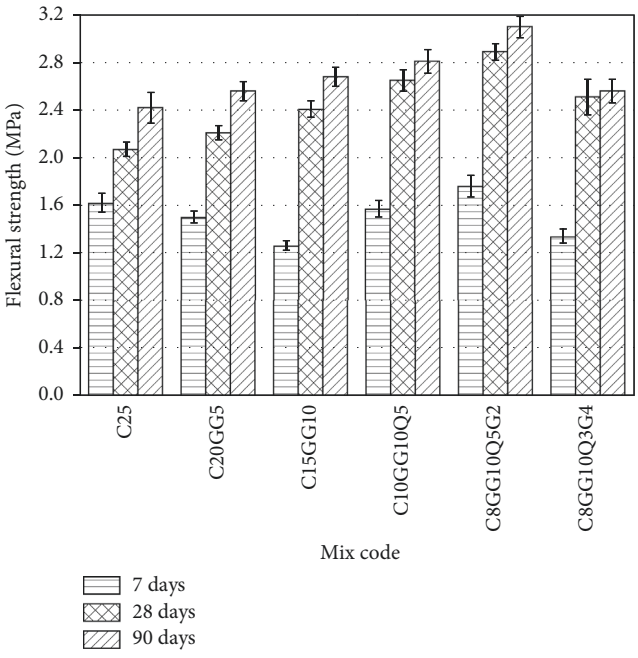

Figure 4: Development of flexural strength of designed mixes.

3. Results and Discussion

3.1. Strength Development of the Unfired Bricks. Figures 3 and 4 present the compressive strength and flexural strength of the

six designed mixes after 7, 28, and 90 days of curing. The compressive strength and flexural strength both increase faster at early ages than at late ages. With the increase of GGBS content from 0% (C25) to 10% (C15GG10), the compressive strength and flexural strength of specimens at 28-day curing period increase from 24.45 MPa to 26.59 MPa and from 2.07 MPa to 2.41 MPa, respectively. The reason for the improved strength may be that the addition of GGBS, with filling spaces between grains of sandy soil and contributing to a better material size distribution, results in lower porosity and thus better mechanical strength [16]. Besides, the siliceous and aluminous materials in GGBS can react with $Ca(OH)_2$ from cement hydration to produce C–S–H and C–A–S–H, which increase over time, occupying more void spaces inside the bricks and creating an increasingly dense structure [17–19].

According to Figure 3, compressive strength of C8GG10Q5G2 reaches the highest value of 19.56 MPa, 31.58 MPa, and 33.36 MPa at 7, 28, and 90 days, respectively. The development of flexural strength of C8GG10Q5G2, as shown in Figure 4, is similar to that of compressive strength. It is rather observable that the appropriate addition of quicklime and gypsum can further enhance the strength. In the stabilized system, the CaO from quicklime may react with water to form $Ca(OH)_2$. During the pozzolanic reaction of GGBS activated by quicklime, hydrate reaction compounds develop because of the concentration of Ca^{2+} and OH^-. In addition, Poon et al. [20] and Gesoglu et al. [21] found that the presence of appropriate gypsum could also accelerate the secondary hydration or pozzolanic reaction of GGBS, which contributes to the continuous generation of cementitious products C–S–H and ettringite and thus promotes the strength development at early ages. As detected by SEM and XRD mentioned in Sections 3.6 and 3.7, respectively, these products fill the pores in the structure and help the bricks to be denser and achieve better mechanical properties [22], aligning with previous published studies [23–27].

However, if the gypsum content increases to 4%, the compressive strength decreases to 15.56 MPa, 26.41 MPa, and 28.36 MPa at 7, 28, and 90 days, respectively, and the flexural strength 1.34 MPa, 2.51 MPa, and 2.56 MPa, respectively, at the corresponding ages. The reason for this phenomenon may be that the excessive gypsum could produce too much ettringite, which results in increased level of internal stress and adversely affects the strength development of the bricks [28].

3.2. The Rate of Water Absorption of the Unfired Bricks. The variation of water absorption rate during the curing period of 7, 28, and 90 days is shown in Figure 5. The water absorption rates of all mixes decrease with increasing age, corresponding with the conclusions of previous literature [22, 29, 30]. James and Rao [31] explained that this was attributed to the transformation of C–S–H gel after prolonged curing into a more crystallized C–S–H. For C8GG10Q5G2, water absorption rate is 8.7%, 2.5%, and 2.3%, the lowest value at the 7-, 28-, and 90-day curing

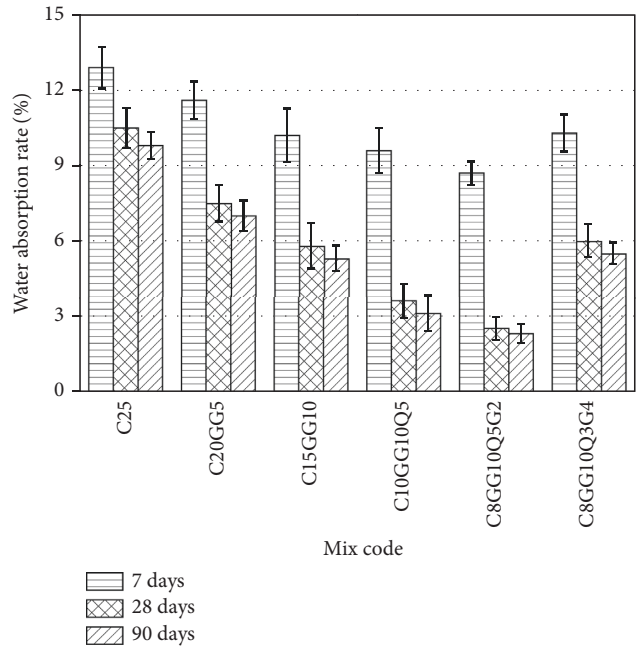

Figure 5: The rate of water absorption with age of designed mixes.

periods, respectively, which decreases by 32.56%, 76.19%, and 76.53% compared with the specimens addition of cement alone at the corresponding ages. This phenomenon has been explained by some researchers [9]. The added GGBS has the capacity of not only correcting particle size distribution, but also modifying sandy soil properties especially at the adequate content of quicklime and gypsum, which benefits the increase of C–S–H and ettringite development accompanied by a decreasing of internal pore size of the brick specimens. Thus, the internal structure of the bricks could be intensive enough to avoid absorption of water.

For C8GG10Q3G4, water absorption rate increases to 10.3%, 6.0%, and 5.5% at the 7, 28, and 90 days, respectively. Gesoglu et al. [21] explained that the excessive gypsum produces a large amount of ettringite, causing the stabilized brick cracks to swell. This swelling effect can disrupt the already established cementitious bonds between sandy soil particles in the stabilized system. According to the study by Miqueleiz et al. [29], the breakdown of chemical bonds between stabilized constituents may create a more open internal structure on the unfired bricks, thus increasing the amount of water infiltrating into C8GG10Q3G4 brick specimens.

3.3. Percentage of Voids of the Unfired Bricks. Figure 6 illustrates the percentage of voids present in the various unfired bricks at the curing age of 7, 28, and 56 days.

It is observed that for C8GG10Q5G2, the percentage of voids drops to 1.56%, 1.22%, and 1.19% after 7, 28, and 56 days of curing, respectively. The results show that the amount of voids has an effect on the overall performance of the stabilized bricks. The compressive strength and flexural strength, for example, increase as the percentage of void space decreases and the specimens of C8GG10Q5G2, with

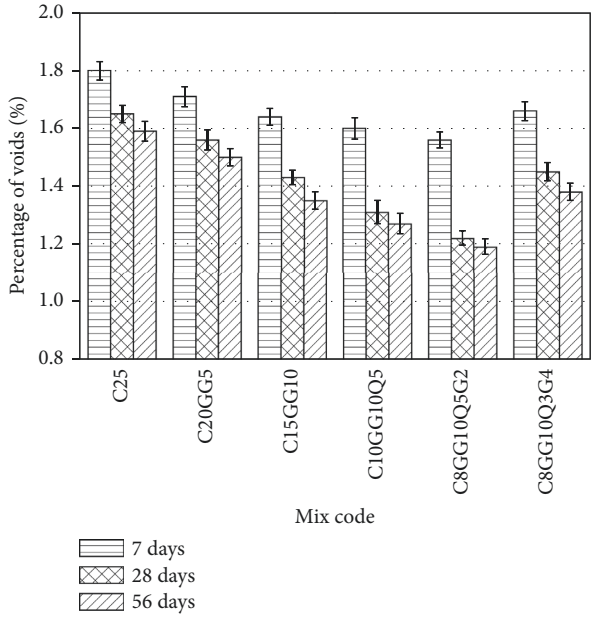

Figure 6: The percentage of voids of designed mixes.

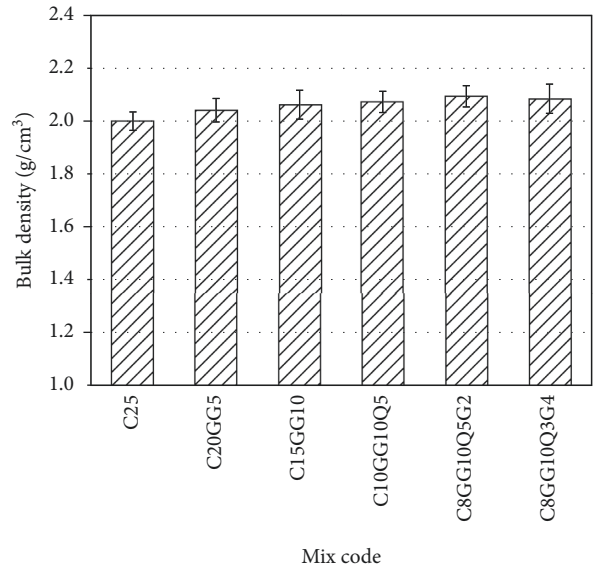

Figure 7: The bulk density of designed mixes.

the lowest percentage of voids, have the highest compressive and flexural strength values. One possible explanation of this phenomenon may be that with the appropriate quicklime and gypsum, the pozzolanic reaction of GGBS can be activated to the fullest, facilitating the appropriate amount of cementitious products C–S–H and ettringite production. These products fill as much void space as possible, instead of displacing the sandy soil particles before filling all the voids in the brick specimens. Besides, Bédérina et al. [32] demonstrated that correction of the granular distribution by appropriate addition of GGBS had allowed minimizing porosity of specimens. As a result, the strength properties, especially for C8GG10Q5G2 further improve.

3.4. Bulk Density of the Unfired Bricks. The results of the bulk density of specimens after 28-day curing age are shown in Figure 7.

It can be seen that the densities for all specimens are very similar within the range of 2.00–2.09 g/cm^3 at 28-day curing period. When replacement content of GGBS varies from 0% (C25) to 10% (C15GG10), density increases from 2.00 g/m^3 to 2.06 g/m^3. Originally, the lower content of GGBS than that

Table 3: The compressive strength and weight loss of the unfired bricks during the freezing/thawing cycles.

Mix code	5 cycles		10 cycles		15 cycles	
	Compressive strength loss (%)	Weight loss (%)	Compressive strength loss (%)	Weight loss (%)	Compressive strength loss (%)	Weight loss (%)
C25	3.7	0.42	5.1	0.61	6.3	0.95
C20GG5	3.4	0.39	4.8	0.57	6.1	0.91
C15GG10	3.1	0.35	4.4	0.52	5.8	0.86
C10GG10Q5	2.9	0.32	3.9	0.46	5.2	0.81
C8GG10Q5G2	2.5	0.29	3.2	0.41	4.1	0.75
C8GG10Q3G4	6.2	1.23	7.6	1.71	9.5	2.44

Table 4: Effect of water immersion aging on compressive strength of designed mixes.

Mix code	C25	C20GG5	C15GG10	C10GG10Q5	C8GG10Q5G2	C8GG10Q3G4
Compressive strength at 28 days (MPa)	24.45	25.14	26.59	28.13	31.58	26.41
Compressive strength after water immersion (MPa)	21.03	22.12	24.46	26.72	30.62	20.86
Coefficient of softening	0.86	0.88	0.92	0.95	0.97	0.79

of cement will decrease the density of specimens. However, the improvement of the grain size distributions and compactness with the incorporation of GGBS ultimately results in a higher density. This observation is in agreement with the results presented in previous works [30]. Furthermore, as cement content decreases at the expense of quicklime and gypsum, the bulk density increases giving evidence for densification. The highest value of 2.09 g/cm^3 is achieved by C8GG10Q5G2, which has the appropriate addition of quicklime and gypsum, allowing suitable C–S–H formations and ettringite fillings in the pores of the brick specimens.

3.5. Freezing/Thawing Cycles of the Unfired Bricks. Table 3 summarizes the record of the percentage compressive strength and weight loss of the unfired brick specimens. In this test, no visual damage is observed as the freezing/thawing cycles progress. According to Table 3, the unfired brick specimens demonstrate a decreasing trend both in compressive strength and weight loss by addicting GGBS, quicklime, and gypsum. For C8GG10Q5G2, the compressive strength and weight loss drop to the lowest value of 4.1% and 0.75% after 15 freezing/thawing cycles, respectively.

The reason for the decreased compressive strength and weight loss can be explained by the results of many previous researches [33–35]. During the freezing/thawing cycles, the pore water changes into ice, and these ices can displace sandy soil particles, disrupting the interlocking of sandy soil particles, dilating the pore volume, and increasing microcracks' size. However, the increased pore volume and propagation of microcracks through the interfacial transition zone between paste and aggregates cannot fully recover due to the existence of cohesion in sandy soil particles at the time that the ices melt [36, 37]. Therefore, the cyclic thawing/freezing process can reduce the compressive strength and weight of the brick specimens. However, some researchers [38, 39] have found that replacing a part of cement by appropriate pozzolanic addition (GGBS) might lead to stronger and denser interfacial transition zone, which reduces propagation of microcracks. In addition, much less water is absorbed into brick specimens and freezes since the pore-filling effect of appropriate GGBS can allow optimizing compactness of the granular skeleton and lowering the porosity. As a result, the enhanced resistance to freezing/thawing has led to a decrease in percentage of compressive strength and weight loss.

3.6. Water Immersion Aging. The water immersion test results are shown in Table 4, including compressive strength before and after water immersion in MPa and coefficient of softening.

As shown in Table 4, the coefficient of softening increases from 0.86 to 0.97 for cement-treated soil after adding GGBS, quicklime, gypsum, or a combination of these stabilizers but decreases sharply to 0.79 once the gypsum content increases to 4%. For C8GG10Q5G2 and C8GG10Q3G4, replacement of 2% quicklime with 2% gypsum decreases significantly the compressive strength at 28 days after water immersion and leads to a significant change in the coefficient of softening. The addition of GGBS, quicklime, and gypsum can ameliorate the ability of cement-treated soil to resist water attack, and this conclusion is well consistent with that of water absorption rate test. This phenomenon is mainly attributed to the pore-filling effect of GGBS due to the spherical shape preventing water entry [36]. With the activation of quicklime and gypsum, the pozzolanic reaction of GGBS and hydrate reaction of cement are accelerated, which produces more C–S–H and ettringite, so the cement–soil mixes stabilized by GGBS, quicklime, and gypsum become much more compact than those without other stabilizers. However, a significant decrease of compressive strength occur while replacing 2% quicklime with 2% gypsum, and the coefficient of softening also drop from 0.97 to 0.79. The reason for the reduction may be that by building up the crystal framework, too much

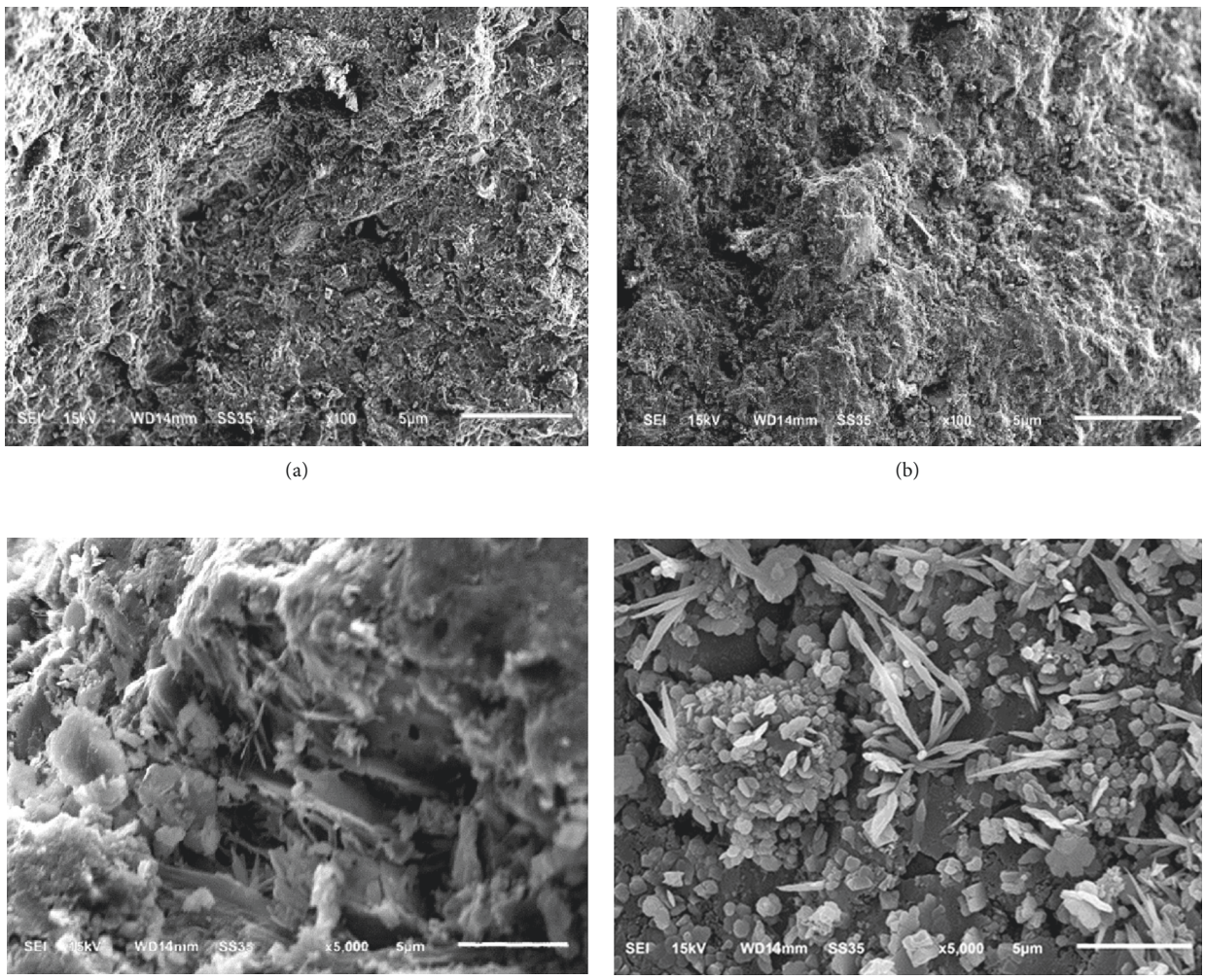

Figure 8: SEM micrographs of C8GG10Q5G2 brick specimens cured for (a) 7 days (×100), (b) 28 days (×100), (c) 7 days (×5000), and (d) 28 days (×5000).

gypsum may expand into the pores and form excessive ettringite, which causes cracks in the structure and has a negative influence on the binding force of sandy soil particles, leading compressive strength to decrease [40].

3.7. SEM Observation. Based on the experimental results discussed above, SEM analysis was conducted on C8GG10Q5G2 brick specimens in order to relate hydrate reaction in the stabilized sandy soil system with strength enhancement. Figure 8 illustrates the SEM imaging information for C8GG10Q5G2 bricks that had been cured for 7 and 28 days, verifying formation of C–S–H and ettringite around the stabilized sandy soil.

It can be observed from Figures 8(a) and 8(b) that the longer curing period lasts the more compacted and continuous the microstructure becomes. When the sandy soil is stabilized with calcium-based binder in the presence of water, the reaction of calcium (from quicklime), alumina (from the sandy soil), and any sulfate present in the system produces C–A–S–H minerals, one of which is ettringite. Also, the C_3S and C_2S present in the cement react with water forming complex C–S–H [9]. On the other hand, pozzolanic reaction of GGBS is accelerated by the activation of quicklime and gypsum. Oti et al. [41] found that these phenomena will promote a more compacted microstructure with less pores, voids, and fractures, as shown in Figure 8(d), resulting from the stronger bonds formed during the hydration process and the possibility of additional pozzolanic C–S–H, and therefore deliver better mechanical and physical properties and durability to the bricks, which is consistent with the data of water absorption, bulk density, and strength development. This agrees with the findings of the research by Peña et al. [42].

3.8. XRD Analysis. In Figure 9, representative XRD diagrams are presented for C8GG10Q5G2 after 7, 28, and 90 days of curing, respectively.

The possible compounds appeared in Figure 9 are products of cement hydration and pozzolanic reaction, including tobermorite C–S–H and portlandite $Ca(OH)_2$. The

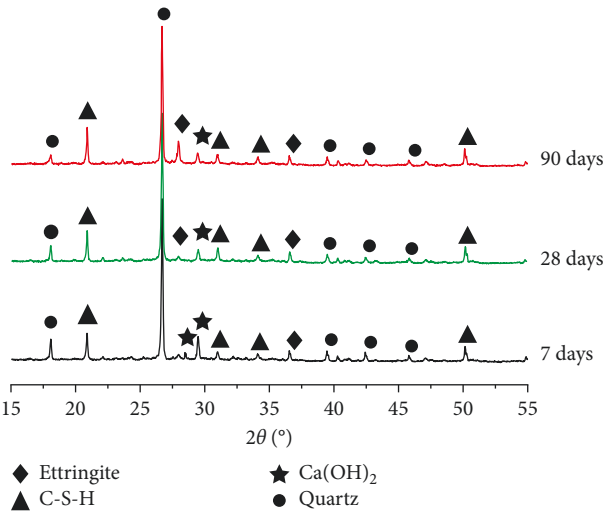

Figure 9: XRD analysis of C8GG10Q5G2 brick specimens cured for 7, 28, and 90 days.

X-ray reflections of C–S–H at 21.3°, 31.6°, 34.0°, and 50.2° (2θ), $Ca(OH)_2$ at 29.4° (2θ), and ettringite at 36.9° (2θ) can be identified. It is noteworthy that the peak of $Ca(OH)_2$ at 28.4° (2θ), identified in brick specimens at the curing period of 7 days, cannot be observed in the specimens cured for 28 days or 90 days. Instead, at 2θ value of 27.9°, ettringite phases can be detected in brick specimens after both 28 days and 90 days of curing. For C8GG10Q5G2, it can be observed that the peaks of C–S–H and ettringite in specimens increase as the curing period increases, which is in good agreement with SEM observation results mentioned previously, which is why the performance of 90-day cured C8GG10Q5G2 specimens are better than that of both 7-day and 28-day cured C8GG10Q5G2 specimens. It can be generally found that the higher the quantity of C–S–H and ettringite the better performance of brick specimens is [36].

4. Conclusions

The results obtained suggest that there is a potential for the use of waste sandy soil as the primary raw material to prepare unfired bricks with excellent mechanical and physical properties and durability. This will facilitate more sustainable brick production. Cement, GGBS, quicklime, and gypsum have all shown a high potential for use as stabilizers in the preparation of unfired bricks. Tests of compressive and flexural strength, rate of water absorption, percentage of voids, bulk density, freezing/thawing, and water immersion resistance as well as SEM and XRD analyses were conducted to investigate the performance of eco-friendly unfired bricks. The following conclusions are therefore drawn from this experimental study:

(1) The strength characteristics of unfired brick specimens can be improved with the incorporation of GGBS, quicklime, and gypsum, compared with the specimens when adding cement alone. For C8GG10Q5G2, the compressive strength and flexural strength at 28-day curing period reach 31.58 MPa and 2.89 MPa, respectively, presenting an acceptable mechanical performance.

(2) The addition of appropriate cement, GGBS, quicklime, and gypsum benefits in enhancing the overall physical properties and durability of unfired bricks. For C8GG10Q5G2, the total overall water absorption rate, percentage of voids, compressive strength and weight loss, and softening coefficient show excellent physical properties and durability of derived bricks.

(3) Results from SEM observation and XRD analysis indicate that there are quite a lot of hydrate products such as C–S–H gel and ettringite binding sandy soil particles together and therefore ameliorating the mechanical and physical behavior and durability of the derived bricks made with sandy soil.

(4) Due to the activating effect of quicklime and accelerating effect of gypsum on the rate of pozzolanic reaction of GGBS, the additional formation of C–S–H gel and ettringite can be furthered favored. In addition, the correction of particle size distribution and pore-filling effects of GGBS contribute to a denser structure of unfired bricks. These result in better mechanical and physical properties and durability.

(5) The utilization of the waste sandy soil to make eco-friendly unfired bricks can reduce land taking and avoid transportation and pollution of waste sandy soil, which would reduce costs such as storage and transportation fee. This study provides a technical approach for the high-efficient comprehensive utilization of waste sandy soil and brings great economic and environmental benefits.

Conflicts of Interest

The authors declare that there are no conflicts of interests regarding the publication of this paper.

Acknowledgments

The work described in this paper was supported by the Natural Science Foundation of China (no. 51409088).

References

[1] M. Boutouil, *Traitement des Vases de Dragage Par Stabilization/Solidification à Base de Ciment et Additifs*, Ph.D. thesis, University of Le Havre, Le Havre, France, 1998.

[2] D. Colin, *Valorisation de Sédiments Fins de Dragage en Technique Routière*, Ph.D. thesis, University of Caen, Caen, France, 2003.

[3] R. Zentar, V. Dubois, and N. E. Abriak, "Mechanical behaviour and environmental impacts of a test road built with marine dredged sediments," *Resources, Conservation and Recycling*, vol. 52, no. 6, pp. 947–954, 2008.

[4] V. Dubois, N. E. Abriak, R. Zentar, and G. Ballivy, "The use of marine sediments as a pavement base material," *Waste Management*, vol. 29, no. 2, pp. 774–782, 2009.

[5] D. X. Wang, N. E. Abriak, R. Zentar, and W. Y. Xu, "Solidification/stabilization of dredged marine sediments for road construction," *Environmental Technology*, vol. 33, no. 1, pp. 95–101, 2012.

[6] B. V. V. Reddy and K. S. Jagadish, "Embodied energy of common and alternative building materials and technologies," *Energy and Buildings*, vol. 35, no. 2, pp. 129–137, 2003.

[7] L. Y. Zhang, "Production of bricks from waste materials—a review," *Construction and Building Materials*, vol. 47, pp. 643–655, 2013.

[8] L. Miqueleiz, F. Ramírez, A. Seco et al., "The use of stabilised Spanish clay soil for sustainable construction materials," *Engineering Geology*, vol. 133-134, pp. 9–15, 2012.

[9] C. H. Weng, D. F. Lin, and P. C. Chiang, "Utilization of sludge as brick materials," *Advance in Environmental Research*, vol. 7, no. 3, pp. 679–685, 2003.

[10] S. Roy, G. R. Adhikari, and R. N. Gupta, "Use of gold mill tailings in making bricks: a feasibility study," *Waste Management and Research*, vol. 25, no. 5, pp. 475–482, 2007.

[11] S. K. Malhotra and S. P. Tehri, "Development of bricks from granulated blast furnace slag," *Construction and Building Materials*, vol. 10, no. 3, pp. 191–193, 1996.

[12] S. Kumar, "A perspective study on fly ash-lime-gypsum bricks and hollow blocks for low cost housing development," *Construction and Building Materials*, vol. 16, no. 8, pp. 519–525, 2002.

[13] F. El Fgaier, Z. Lafhaj, C. Chapiseau, and E. Antczak, "Effect of sorption capacity on thermo-mechanical properties of unfired clay bricks," *Journal of Building Engineering*, vol. 6, pp. 86–92, 2016.

[14] W. H. Wang, L. H. Han, W. Li, and Y. H. Jia, "Behavior of concrete-filled steel tubular stub columns and beams using dune sand as part of fine aggregate," *Construction and Building Materials*, vol. 51, pp. 352–363, 2014.

[15] O. Plé and T. N. H. Lê, "Effect of polypropylene fiber-reinforcement on the mechanical behavior of silty clay," *Geotextiles and Geomembranes*, vol. 32, pp. 111–116, 2012.

[16] J. J. Chauvin and G. Grimaldi, "Les bétons de sable," *Bulletin de Liaison Laboratoires des Ponts et Chaussées (LCPC)*, vol. 157, pp. 9–15, 1998, in French.

[17] A. Fernández-Jimćnez, A. Palomo, and M. Criado, "Microstructure development of alkali-activated fly ash cement: a descriptive model," *Cement and Concrete Research*, vol. 35, no. 6, pp. 1204–1209, 2005.

[18] J. Tangpagasit, R. Cheerarot, C. Jaturapitakkul, and K. Kiattikomol, "Packing effect and pozzolanic reaction of fly ash inmortar," *Cement and Concrete Research*, vol. 35, no. 6, pp. 1145–1151, 2005.

[19] C. L. Hwang and T. P. Huynh, "Evaluation of the performance and microstructure of ecofriendly construction bricks made with fly ash and residual rice husk ash," *Advances in Materials Science and Engineering*, vol. 2015, pp. 1–11, 2015.

[20] C. S. Poon, S. C. Kou, L. Lam, and Z. S. Lin, "Activation of fly ash/cement systems using calcium sulfate anhydrite ($CaSO_4$)," *Cement and Concrete Research*, vol. 31, no. 6, pp. 873–881, 2001.

[21] M. Gesoglu, E. Güneyisi, A. H. Nahhab, and H. Yazıcı, "The effect of aggregates with high gypsum content on the performance of ultra-high strength concretes and Portland cement mortars," *Construction and Building Materials*, vol. 110, pp. 346–354, 2016.

[22] J. E. Oti, J. M. Kinuthia, and J. Bai, "Engineering properties of unfired clay masonry bricks," *Engineering Geology*, vol. 107, no. 3-4, pp. 130–139, 2009.

[23] C. K. Yip, G. C. Lukey, and J. S. J. vanDeventer, "The coexistence of geopolymeric gel and calcium silicate hydrate at the early stage of alkaline activation," *Cement and Concrete Research*, vol. 35, no. 9, pp. 1688–1697, 2005.

[24] M. H. Zhang, R. Lastra, and V. M. Malhotra, "Rice-husk ash paste and concrete: some aspects of hydration and the microstructure of the interfacial zone between the aggregate and paste," *Cement and Concrete Research*, vol. 26, no. 6, pp. 963–977, 1996.

[25] R. Zejak, I. Nikolić, D. Blečić, V. Radmilović, and V. Radmilović, "Mechanical and microstructural properties of the fly-ash based geopolymer paste and mortar," *Material in Technology*, vol. 47, no. 4, pp. 535–540, 2013.

[26] K. Ogawa and D. M. Roy, "C_4A_3S hydration, ettringite formation, and its expansion mechanism: microstructural observation of expansion," *Cement and Concrete Research*, vol. 12, no. 1, pp. 101–109, 1982.

[27] H. Uchikawa and S. Uchida, "Influence of character of blending component on the diffusion of Na and Cl ions in hardened blended cement paste," *Journal of Research of the Onoda Cement Company*, vol. 39, no. 5, pp. 245–250, 1986.

[28] C. H. Jiang, X. B. Zhou, G. L. Tao, and D. Chen, "Experimental study on the performance and microstructure of cementitious materials made with dune sand," *Advances in Materials Science and Engineering*, vol. 2016, pp. 1–8, 2016.

[29] L. Miqueleiz, F. Ramirez, J. E. Oti et al., "Alumina filler waste as clay replacement material for unfired brick production," *Engineering Geology*, vol. 163, pp. 68–74, 2013.

[30] M. S. El-Mahllawy and A. M. Kandeel, "Engineering and mineralogical characteristics of stabilized unfired montmorillonitic clay bricks," *Applied Clay Science*, vol. 118, no. 1, pp. 171–177, 2015.

[31] J. James and S. Rao, "Reaction product of lime and silica from rice husk ash," *Cement and Concrete Research*, vol. 16, no. 1, pp. 67–73, 1986.

[32] M. Bédérina, M. M. Khenfer, R. M. Dheilly, and M. Quéneudec, "Reuse of local sand: effect of limestone filler proportion on the rheological and mechanical properties of different sand concretes," *Cement and Concrete Research*, vol. 35, no. 6, pp. 1172–1179, 2005.

[33] G. R. Benoit and W. B. Voorhees, "Effect of freeze-thaw activity on water retention, hydraulic conductivity, density and surface strength of two soils frozen at high water content," in *Proceedings of the International Symposium, Frozen Soil Impacts on Agricultural, Range and Forest Lands* Special USA Cold Regions Research and Engineering Laboratory, Special Report 90–91, Spokane, WA, USA, March 1990.

[34] O. B. Andersland and B. Ladanyi, *Frozen Ground Engineering*, American Society of Civil Engineers and John Wiley & Sons (ASCE Press), New York, NY, USA, 2nd edition, 2004.

[35] Z. H. Liu, Q. Y. Chen, X. B. Xie et al., "Utilization of the sludge derived from dyestuff-making wastewater coagulation for unfired bricks," *Construction and Building Materials*, vol. 25, no. 4, pp. 1699–1706, 2011.

[36] R. Zentar, D. X. Wang, N. E. Abriak, M. Benzerzour, and W. Z. Chen, "Utilization of siliceous-aluminous fly ash and cement for solidification of marine sediments," *Construction and Building Materials*, vol. 35, pp. 856–863, 2012.

[37] M. Vancura, K. MacDonald, and L. Khazanovich, "Microscopic analysis of paste and aggregate distresses in pervious concrete in a wet, hard freeze climate," *Cement and Concrete Composites*, vol. 33, pp. 1080–1085, 2011.

[38] M. Nili and A. Ehsani, "Investigating the effect of the cement paste and transition zone on strength development of

concrete containing nanosilica and silica fume," *Materials and Design*, vol. 75, pp. 174–183, 2015.

[39] P. Duan, Z. Shui, W. Chen, and C. Shen, "Effects of metakaolin, silica fume and slag on pore structure, interfacial transition zone and compressive strength of concrete," *Construction and Building Materials*, vol. 44, pp. 1–6, 2013.

[40] P. Zak, T. Ashour, A. Korjenic, S. Korjenic, and W. Wu, "The influence of natural reinforcement fibers, gypsum and cement on compressive strength of earth bricks materials," *Construction and Building Materials*, vol. 106, pp. 179–188, 2016.

[41] J. E. Oti, J. M. Kinuthia, and J. Bai, "Compressive strength and microstructural analysis of unfired clay masonry bricks," *Engineering Geology*, vol. 109, no. 3-4, pp. 230–240, 2009.

[42] P. P. Peña, M. A. G. Lozano, A. R. Pulido et al., "Effect of crushed glass cullet sizes on physical and mechanical properties of red clay bricks," *Advances in Materials Science and Engineering*, vol. 2016, pp. 1–5, 2016.